



Binding site feature description of 2-substituted benzothiazoles as potential AcrAB-TolC efflux pump inhibitors in *E. coli*

S. Yilmaz, G. Altinkanat-Gelmez, K. Bolelli, D. Guneser-Merdan, M. Ufuk Over-Hasdemir, E. Aki-Yalcin & I. Yalcin

To cite this article: S. Yilmaz, G. Altinkanat-Gelmez, K. Bolelli, D. Guneser-Merdan, M. Ufuk Over-Hasdemir, E. Aki-Yalcin & I. Yalcin (2015) Binding site feature description of 2-substituted benzothiazoles as potential AcrAB-TolC efflux pump inhibitors in *E. coli*, SAR and QSAR in Environmental Research, 26:10, 853-871

To link to this article: <http://dx.doi.org/10.1080/1062936X.2015.1106581>



Published online: 12 Nov 2015.



Submit your article to this journal [↗](#)



View related articles [↗](#)



View Crossmark data [↗](#)

Binding site feature description of 2-substituted benzothiazoles as potential AcrAB-TolC efflux pump inhibitors in *E. coli*[§]

S. Yilmaz^a, G. Altinkanat-Gelmez^b, K. Bolelli^a, D. Guner-Merdan^b,
M. Ufuk Over-Hasdemir^b, E. Aki-Yalcin^a and I. Yalcin^{a*}

^aPharmaceutical Chemistry Department, Faculty of Pharmacy, Ankara University, Ankara, Turkey;

^bMedical Microbiology Department, Faculty of Medicine, Marmara University, Istanbul, Turkey

(Received 20 July 2015; in final form 7 October 2015)

The resistance-nodulation-division (RND) family efflux pumps are important in the antibiotic resistance of Gram-negative bacteria. However, although a number of bacterial RND efflux pump inhibitors have been developed, there has been no clinically available RND efflux pump inhibitor to date. A set of BSN-coded 2-substituted benzothiazoles were tested alone and in combinations with ciprofloxacin (CIP) against the AcrAB-TolC overexpressor *Escherichia coli* AG102 clinical strain. The results indicated that the BSN compounds did not show intrinsic antimicrobial activity when tested alone. However, when used in combinations with CIP, a reversal in the antibacterial activity of CIP with up to 10-fold better MIC values was observed. In order to describe the binding site features of these BSN compounds with AcrB, docking studies were performed using the CDocker method. The performed docking poses and the calculated binding energy scores revealed that the tested compounds BSN-006, BSN-023, and BSN-004 showed significant binding interactions with the phenylalanine-rich region in the distal binding site of the AcrB binding monomer. Moreover, the tested compounds BSN-006 and BSN-023 possessed stronger binding energies than CIP, verifying that BSN compounds are acting as the putative substrates of AcrB.

Keywords: AcrAB-TolC; AcrB docking; benzothiazoles; ciprofloxacin; *E. coli* AG102; EPI

1. Introduction

Multidrug resistance (MDR) of human pathogenic bacteria is an emerging problem for global public health [1]. Bacterial efflux pumps, which cause drug extrusion, serve as an important mechanism of MDR among the general mechanisms of antibiotic resistance including target alteration, drug inactivation, and decreased permeability of bacterial cell. The resistance mediated by the efflux pumps is often associated with the overproduction of membrane transport proteins, which are able to pump antibiotics, chemotherapeutics, detergents, dyes, toxins, and organic solvents out of the bacterial cell [2–5]. Besides owing a broad range of antibiotic resistance to their poly-substrate specificity, efflux pumps also drive additional resistance mechanisms by lowering intracellular antibiotic concentration and elevating mutation accumulation [6].

*Corresponding author. Email: yalcin@ankara.edu.tr

[§]Presented at the 8th International Symposium on Computational Methods in Toxicology and Pharmacology Integrating Internet Resources, CMTPI-2015, June 21–25, 2015, Chios, Greece.

Bacterial efflux pumps are found in almost all bacterial species, and they are classified into five families according to their composition (number of transmembrane-spanning regions, energy sources and substrates) [7–10]. Depending on the specific classes they belong to, the resistance-nodulation-division (RND) family pumps, which are only found in Gram-negative bacteria, have a tripartite composition. RND-type efflux pumps contain an inner membrane transporter protein (RND pump), an outer membrane protein (OMP) channel, and a periplasmic membrane fusion protein (MFP) [1,11], which allow direct extrusion of various antibiotics from the cytosol or periplasmic space to the outside of the bacterial cell, and have been found to be associated extensively with clinically significant antibiotic resistance [4,8].

In the Gram-negative bacterium *Escherichia coli*, the tripartite efflux system AcrAB-TolC is in charge of the efflux of multiple antibiotics including chloramphenicol, beta lactam antibiotics, tetracycline, novobiocin, rifampin, fusidic acid, nalidixic acid and fluoroquinolones [3,4,8]. As an example, a high level of fluoroquinolone resistance in 50 screened clinical *E. coli* strains isolated from human clinical samples in Sapporo, Japan, revealed a strong correlation with the overexpression of the AcrAB efflux pumps [12]. Overexpression of MDR efflux pumps, which causes resistance against several different classes of antibiotics by increasing their minimum inhibitory concentration (MIC) values, has been frequently found in clinical isolates. Recent studies suggested that MDR efflux transporters have a major role in the efficacy of both new and old antibiotics [13].

As shown in Figure 1(a), the tripartite AcrAB-TolC RND efflux pump system in *E. coli* possesses a transporter protein (RND pump) AcrB acting as a proton/drug antiporter, an outer membrane channel protein TolC, and a periplasmic membrane fusion protein AcrA, which serves as a linker between TolC and AcrB [1,3,4,14]. The newly elucidated asymmetric structure of trimeric AcrB reveals three different monomer conformations representing consecutive states in a transport cycle (Figure 1(b)). The monomers show tunnels with occlusions at different sites, and the structural changes create a hydrophobic deep binding pocket in one monomer (binding monomer), which is not present in the other two monomers at the functional rotation transport mechanism [2–4]. Minocycline, doxorubicin, and ciprofloxacin (CIP) are AcrB substrates, and specifically bind to this deep binding site, substantiating its role as drug-binding pocket [3,4,15].

Studies on the structures of RND efflux pumps have not only provided essential evidence for the mechanisms of multidrug binding and extrusion, but have also shed light on the structure-based approach to discover RND efflux pump inhibitors (EPIs). Several classes of EPIs, such as peptidomimetics and arylpiperazines, have been extensively characterized to date [1,4,13,16,17]. Phenylalanyl arginyl *beta*-naphthylamide (PA β N) was the first identified peptidomimetic, which inhibits *P. aeruginosa* efflux systems [2,4,16–18], and it successfully reduced the emergence of levofloxacin resistance in a *P. aeruginosa* strain [19]. PA β N also shows activity against the AcrAB-TolC efflux system in *E. coli* [3,4,16,18]. PA β N was described as being not an inhibitor of RND efflux pumps, but rather a competitor [20]. Recently, new data has shown that it acts as an inhibitor of AcrAB and AcrEF efflux systems when used in low concentrations. At higher concentrations this compound showed not only inhibitory activity towards the mentioned efflux pumps, but also an effect in destabilizing the outer cell membrane [1,21], and in many cases the observed antibiotic synergism of PA β N could be attributed to non-specific damage to the bacterial membrane [1]. Therefore, the general use of this molecule remains questionable because of the induction of undesirable resistance profiles by reducing drug penetration [3].

Arylpiperazines are the other type of RND inhibitors that could be used to target efflux pumps [1,22]. Specifically, 1-(1-naphthylmethyl)-piperazine (NMP) was found as the most

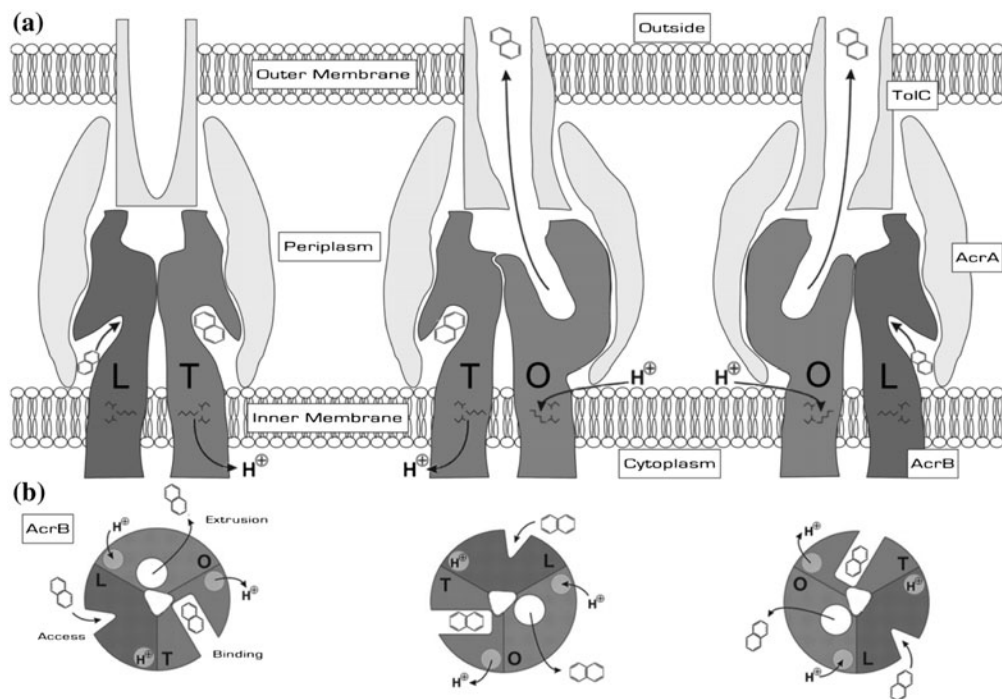


Figure 1. Schematic representations of the RND AcrAB-TolC efflux pump with the view of different conformational stages of the ligand extrusion mechanism in AcrB. (a) Side view schematic representation of tripartite structure of the RND AcrAB-TolC efflux pump system viewing the locations of AcrB, AcrA and TolC proteins. (b) Top view schematic representation of the AcrB three monomers (protomers) that demonstrates the alternating site functional rotation stages of the transport mechanism. In the first stage of the cycle, the monomer representing as the loose (L) conformation, which is defined as the access monomer, possesses a passage that permits potential substrates to enter the protomer. The other monomer has the tight (T) conformation stage, which is named as the binding monomer, and comprises the binding pocket in the interior of the periplasmic porter domain that achieves the binding of potential substrate to the hydrophobic binding pocket. Finally, the monomer representing as the open (O) conformation, which is defined as the extrusion protomer, releases the substrate in the funnel toward TolC. The conversion from the O conformation stage to the L conformation is a proton-motive force-dependent step and requires a proton from the periplasm. The conversion from the T monomer stage to the O monomer is accompanied by the release of a proton to the cytoplasm. This figure is adapted from Misra and Bavro [61].

potent EPI active compound among the other derivatives of arylpiperazines, and exhibits an enhanced action for the accumulation of several antibiotics in the intracellular region of the RND efflux pump overexpressor bacterial cell [4,23,24]. However, arylpiperazine derivatives were found to be toxic for clinical use because of their 'serotonin agonist' properties [3,17]. Even though significant efforts have been realized in the development of EPIs to date, none of these EPIs are suitable for use in clinics currently. One main reason is that the mechanisms of action of most EPIs remain unknown.

Recently, the BSN-coded 2-substituted benzothiazoles were synthesized and tested by our research group in combinations with ciprofloxacin (CIP) against the *A. baumannii* SbMox-2 clinical isolate, which is an AdeABC RND efflux pump overexpressor. Some of

our synthesized benzothiazole derivatives supplied reversal of the antibacterial activity of CIP against the AdeABC overexpressor *A. baumannii* strain, contributing sensitivity on the MIC value of CIP of 20-fold double dilution better antibacterial activity, providing a MIC value below the EUCAST susceptibility MIC breakpoint for CIP versus *Acinetobacter spp.* for use in clinical treatment [25]. The generated 3D-common feature pharmacophore hypothesis revealed that the conformational properties of the compounds were significant for the AdeABC efflux pump inhibitory activity against the MDR *A. baumannii* SbMox-2 strain, and compounds possessing 2-[4-(4-substituted-2-phenyl-acetamido)phenyl]benzothiazole and/or 2-[4-(4-substituted-3-phenylpropionamide)-phenyl]benzothiazole structures were found important for improving the AdeABC efflux pump inhibitor potency, rather than the 2-[4-(4-substitutedbenzamido)benzyl]benzothiazole structure in these tested 2-substituted benzothiazoles.

MDR can be considered as the new challenge for the 21st century⁴⁸, and the increased level of MDR to antimicrobial agents has revealed serious problems in the treatment of pathogens [26]. Global organizations, initially such as the World Health Organization, have designated their concern on this issue, suggesting that increased focus and efforts are required to address this challenge [27]. In particular, the emergence of MDR strains of Gram-negative bacteria pathogens such as the RND-type AcrAB-TolC efflux pump overexpressor clinical isolate of *E. coli* is a problem of ever increasing significance [4]. Interestingly, this efflux pump decreases the antibacterial activity of dissimilar antibiotic structures, which can be considered a MDR mechanism [11]. Because bacteria become insensitive to different classes of antibiotic therapy, new therapeutic approaches must be looked for, with new molecules to block efflux, to restore drug susceptibility to resistant clinical strains.

The goal of the present study is (i) to observe the EPI activity of the previously synthesized BSN-coded 2-substituted benzothiazoles to develop potential new AcrAB-TolC efflux pump inhibitors in *E. coli*, to reverse the antibacterial activity of antibiotics, particularly CIP, in the AcrAB-TolC efflux pump overexpressor *E. coli* AG102 clinical isolate, and (ii) to examine the structure–activity relationships by describing the binding site features of these BSN-coded 2-substituted benzothiazole derivatives on RND efflux pump protein (AcrB) in *E. coli* by using molecular docking studies.

2. Materials and methods

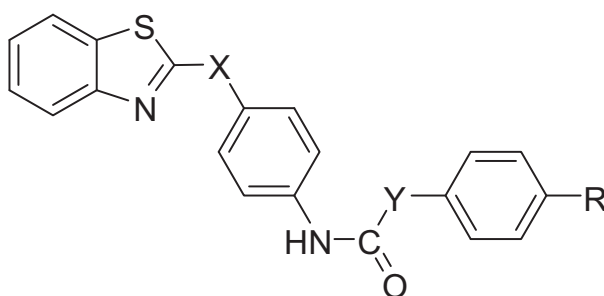
2.1 Tested compounds

In order to investigate the bacterial RND-type AcrAB-TolC efflux pump inhibitory activity in the *E. coli* AG102 isolate, we tested our 14 previously synthesized BSN-coded 2-substituted benzothiazole derivatives fused heterocyclic compounds [28,29], which hold different atoms and/or atom groups on X, Y, and R positions in their structure, as shown in Table 1.

2.2 Bacterial strain

The RND-type AcrAB-TolC efflux pump overexpressor clinical isolate *E. coli* AG102 [30–34] was tested. The tested strain *E. coli* AG102 was previously derived from AG100 [30,32] and it is MDR due to a mutation in MarR (*marR1*), which increases the expression of MarA, a global regulator in the overexpression of the AcrAB-TolC efflux system [31,33–36]. The test strain was grown overnight at 37°C in Mueller Hinton Broth (MHB) (Oxoid, UK).

Table 1. The structures of the tested BSN coded 2-substituted benzothiazoles.



Compound code	R	X	Y
BSN-001	H	-	-
BSN-002	OCH ₂ (CH ₂) ₂ C ₂ H ₅	-	-
BSN-003	C ₂ H ₅	-	-
BSN-004	OCH ₃	-	CH ₂
BSN-005	F	-	CH ₂
BSN-006	CH ₃	-	CH ₂
BSN-008	H	-	CH ₂
BSN-010	F	CH ₂	CH ₂
BSN-016	F	CH ₂	-
BSN-017	Br	CH ₂	-
BSN-018	NO ₂	CH ₂	-
BSN-019	C ₂ H ₅	CH ₂	-
BSN-020	H	CH ₂	-
BSN-023	H	-	C ₂ H ₄

2.3 Susceptibility testing

A standard microdilution assay was used to determine the MIC of our previously synthesized BSN-coded compounds and CIP (Sigma-Aldrich, US) [37]. The BSN-coded compounds were dissolved in dimethyl sulfoxide (DMSO) and the two-fold serial dilutions were prepared using cation-adjusted MHB at a concentration range between 512 µg/ml and 0.0625 µg/ml. Direct colony suspension of the tested bacteria from the fresh cultures was prepared in order to have a turbidity equivalent to 0.5 McFarland standard. The inoculum suspension was then diluted in MHB to give a final cell number of 5×10^5 cfu/ml. The final concentration of the inoculum was added to two-fold serial dilution of the compounds. The microdilution trays were incubated at $35 \pm 2^\circ\text{C}$ for 16–20 h in an ambient air incubator.

MICs of CIP were determined in the presence and absence of the BSN-coded compounds. Half of the concentrations of the observed MIC values (2-fold dilution lower than the MIC) of the tested BSN-coded compounds was added into broth microdilution wells in combinations with CIP considered as having a non-inhibitory effect on bacterial growth. An 8-fold or greater reduction in the MIC value of CIP after addition of BSN-coded fused heterocyclic compounds, which comprises a MIC value of ≤ 0.008 µg/ml providing the European Committee on Antimicrobial Susceptibility Testing (EUCAST AST guidelines Version 1.3 December 2010) MIC susceptibility breakpoint for CIP versus *E. coli* ATCC 25922 strain for use in clinical treatment [38], was considered as a potential EPI. All susceptibility tests were performed twice. The observed MIC values of CIP, the tested BSN-coded compounds alone, and the combinations with CIP against AcrAB-TolC efflux pump overexpressor *E. coli* AG102 clinical isolate are given in Table 2.

Table 2. Observed MIC values of ciprofloxacin (CIP) and BSN-coded 2-substituted benzothiazoles as tested alone and in combinations against the AcrAB-TolC efflux pump overexpressor *Escherichia coli* AG102 strain.

<i>Compound code</i>	<i>MIC (µg/ml)^a</i>	<i>Escherichia coli AG102 Combination with CIP</i>	<i>MIC (µg/ml)^b</i>
CIP	0.125		
BSN-001	256	CIP+ BSN-001	0.03
BSN-002	64	CIP+ BSN-002	0.5
BSN-003	128	CIP+ BSN-003	0.016
BSN-004	256	CIP+ BSN-004	0.008
BSN-005	128	CIP+ BSN-005	0.03
BSN-006	512	CIP+ BSN-006	0.004
BSN-008	256	CIP+ BSN-008	0.125
BSN-010	256	CIP+ BSN-010	0.03
BSN-016	128	CIP+ BSN-016	0.03
BSN-017	128	CIP+ BSN-017	0.03
BSN-018	128	CIP+ BSN-018	0.06
BSN-019	64	CIP+ BSN-019	0.06
BSN-020	256	CIP+ BSN-020	0.016
BSN-023	512	CIP+ BSN-023	0.004

^aObserved MIC values of compounds tested alone.

^bObserved MIC values of CIP tested in combination with BSN compounds.

2.4 Computational methods

2.4.1 Molecular structures and optimization

The 3D structures of a set of previously synthesized BSN-coded 2-substituted benzothiazole derivatives, which are given in Table 1 [22,23], as well as the antibiotics minocycline, doxorubicin, and CIP were sketched using the Discovery Studio (DS) 3.5 [39] Sketch Molecules module. The geometries of these compounds were subsequently optimized using the Minimization module of DS 3.5 using the CHARMM (Chemistry at Harvard Macromolecular Mechanics) force field. CHARMM provides a vast range of functionality for molecular mechanics and can be used to diverse areas of research, including protein modelling and structural biology [40].

2.4.2 Molecular docking

The most straightforward computational approaches for finding new leads for therapeutic macromolecular targets are increasingly based on 3D information about proteins. Molecular docking is an effective method to predict ligands, which are low molecular weight compounds that may interact with a macromolecular target [41]. A primary objective in molecular docking is the ability to estimate the scoring function and evaluate protein–ligand interactions as a means of hit identification (virtual screening) and lead optimization (to enhance desired drug properties). This method is also successfully used as a computational tool to assist drug discovery.

2.4.2.1 Preparation of the transporter. The crystal structure of AcrB (PDB ID: 2DRD) was retrieved from the Protein Data Bank (PDB) (www.rcsb.org) [15] and further modified for docking calculations. For preparation of protein and ligands, DS 3.5 software was used. The

target protein was taken, hydrogens were added and their positions were optimized using the all-atom CHARMM force field and the Adopted Basis set Newton Raphson (ABNR) method available in the DS 3.5 protocol until the root mean square deviation (RMSD) gradient was $<0.05 \text{ kcal mol}^{-1} \text{ \AA}^{-2}$. The minimized protein was defined as the receptor using the binding site module. The binding site was defined from the current selection method by using the DS 3.5 protocol, which was modified to accommodate all the important interacting residues at the binding site of AcrB porter domain due to the resolved crystal structure of AcrB with its substrate, minocycline.

2.4.2.2 Preparation of ligands. BSN-coded 2-substituted benzothiazole derivatives, minocycline, doxorubicin, and ciprofloxacin were sketched, and all-atom CHARMM force field parameterization was assigned and then minimized using the ABNR method as described above. Conformational searches of the ligands were carried out using a simulated annealing molecular dynamics (MD) approach. The ligands were heated at a temperature of 700 K and then annealed to 200 K.

2.4.2.3 Core-constrained docking (CCD) subprotocol. The CCD subprotocol includes conformer generation, core-constrained docking and scoring. In terms of core-constrained docking, use of the molecular docking algorithm CDocker is considered since it has been shown to be a viable research tool [42,43]. CDocker is a CHARMM-based grid-enabled docking method that uses soft core potentials and MD-generated random ligand conformations, and poses refinement in the active site using a simulated annealing process. In the original work, CDocker treats the entire ligand as flexible during the initial docking phase. The core-constrained docking method described here is a modification to the CDocker CHARMM script that allows the scaffold to be locked but the rest of the ligand molecule to be flexible during initial minimization and the MD conformer generation stage. The core is allowed to move during final refinement with simulated annealing. Current docking tools do a reasonable job at getting correct poses, but errors occur in a significant number of cases [44,45]. Constraining the core to the crystal structure coordinates helps prevent incorrect docking poses. A grid is defined using the 'Grid Extension' parameter visible at the top level of the subprotocol and has been set to a default 8 Å distance from the ligand's centre of mass. Details of the modified CDocker process begin with creation of the CHARMM set-up files and generation of the CDocker protein grid. Ligand partial atomic charges and atom types default to those of Momany-Rone force field [46] as implemented in CHARMM. The typed ligand is first run through an ABNR minimization stage [40]. Ligand conformations are then generated, in the absence of protein, through high-temperature MD simulations and a specified number (top-level parameter, default = 20) of simulations are applied. The starting ligand conformation for each MD simulation is that of its predecessor. Conformations resulting from each MD simulation are then docked into the protein and minimized using steepest-descent (SD), preparing them for final refinement. It is only during this initial docking and conformer refinement phase that an energy grid for the ligand is imposed and nonbonded interactions involving van der Waals and electrostatic potentials are softened, enabling enhanced sampling of conformational space. The core is held fixed throughout the conformer generation and docking phase. With the core now unconstrained, the docked poses are then further refined in the receptor active site using a simulated annealing protocol and a full MD minimization (SD + conjugate-gradient). During this process the protein is held rigid. A user-specified number of top poses (top-level parameter), based on the largest minus CDocker scores, and are saved

for the final rescoring step. Many of the advanced CHARMM parameters have been optimized and do not require changing from their default values.

The docking parameters were as follows: Top Hits: 10; Random Conformations: 10; Random Conformations Dynamics Step: 1000; Grid Extension: 8.0; Random Dynamics Time Step: 0.002. The docking and scoring methodology was first validated by docking of the known substrates: minocycline, doxorubicin, and CIP. Afterward, molecular docking studies were performed on the tested BSN compounds.

2.4.2.4 Calculated binding energy (CBE) subprotocol. The CDocker docked ligands are rescored using a physics-based implicit solvation model as the final step. Within the CBE subprotocol step, the docked ligand poses are rank scored in terms of their binding energies. For this study, top CDocker poses of neutral and/or charged ligands were rescored using Molecular Mechanics-Generalized Born with Molecular Volume (MM-GBMV) and/or Molecular Mechanics-Generalized Born with Simple Switching (MM-GBSW) methods in DS CHARMM, which approximates the binding energy [47–49]. Bound and unbound ligand receptor energy terms contained within the CBE include three simulations: free ligand; apoprotein; and protein–ligand complex. Solute entropy contributions are ignored in these calculations. Standard output includes the binding energy terms for the three simulations and the net CBE as shown in Equation (1):

$$\Delta G_{\text{Bind}} = \Delta G_{\text{Complex}} - \Delta G_{\text{Ligand}} - \Delta G_{\text{Protein}} \quad (1)$$

In the present study, the CDocker method [42] was performed using DS 3.5. All docked poses were scored by applying the Analyze Ligand Poses subprotocol to analyse receptor–ligand interactions or a set of poses (the results of a docking run) using a variety of methods. Binding energies were also calculated by applying the CBE subprotocol in DS 3.5 using the in situ ligand minimization step (ABNR method) and using generalized born molecular volume model (GBMV). The lowest binding energy was taken as the best-docked conformation of the compound for the macromolecule. The docking results are given in Table 3.

3. Results and discussion

3.1 Microbiological activity

Substituted benzothiazoles and their analogues such as benzoxazoles and benzimidazoles, which are the structural isosteres of nucleotides owing to fused heterocyclic nuclei in their structure, have been the aim of many researchers for many years, because they constitute an important class of heterocyclic compounds with antitumour [41,50,51], antiviral [52], and antimicrobial activities [25,53]. Recent observations suggest that these fused heterocyclic compounds possess potential chemotherapeutic activity with lower toxicities [54,55], and they are in harmony with the Lipinski's rule of five [56].

These observations provided us some predictions to design and evaluate novel lead compounds that are active as RND-type EPs to reverse the antibacterial activity of antibiotics against MDR Gram-negative bacteria such as RND-type AcrAB-TolC efflux pump overexpressing *E. coli*.

For the antibacterial activity test against *E. coli* AG102 clinical isolate, which is an AcrAB-TolC efflux pump overexpressor, BSN-coded 2-substituted benzothiazoles were first tested alone, and it was observed that they did not exhibit any significant intrinsic antibacterial activity, showing MIC values between 64 and 512 µg/ml. But when they were tested at

Table 3. Docking results.

Compound code	E_{bind} [kcal/mol]	Interacting residues ^[a]
BSN-001	-10.7338	Ser134, Ser135, Gln176 (2.42 Å), Leu177, Phe178 ^[b,b] , Gly179, Ser180, Glu273, Asn274, Ile277, Phe615, Phe628 ^[b]
BSN-002	24.7148	Ser48, Tyr49, Pro50, Thr85, Thr87, Gln125, Ser135, Gln176, Phe178, Asn274, Asp276, Ile277, Val612, Phe615, Arg620 ^[c] , Phe628, Tyr772
BSN-003	-8.42626	Ser48, Pro50, Thr85, Gly86, Thr87, Gln176, Phe178, Asn274, Asp276, Ile277, Val612, Phe615 ^[b,b] , Arg620 (1.33 Å, 1.94 Å), Phe628
BSN-004	-7.68639	Ser48, Tyr49, Pro50, Gly51, Thr87, Gln176, Leu177, Phe178 ^[b] , Gly179, Asn274 (2.73 Å), Asp276, Ile277, Phe615, Arg620, Phe628
BSN-005	-8.47374	Ser134, Ser135, Gln176, Leu177, Phe178, Gly179, Ser180, Glu273, Asn274, Ile277, Val612, Phe615 ^[b,b] , Phe628 ^[b]
BSN-006	-17.9724	Ser48, Pro50, Gln125, Gln176, Phe178, Gly179, Ser180, Arg185, Glu273, Asn274 (2.49 Å), Ile277, Ala279, Val612, Gly755, Gly756, Tyr772 ^[b] , Met774
BSN-008	13.0229	Ala47, Ser48, Tyr49, Pro50, Thr85, Gly86, Thr87, Gln125, Leu177, Phe178, Gly179, Asn274, Asp276, Ile277 ^[d] , Val612, Phe615, Arg620 ^[c] , Tyr772
BSN-010	-5.94382	Ser48, Gln125, Phe178, Gly179, Glu273, Asn274, Ile277, Ala279, Val612, Phe615, Phe628, Lys770 (1.78 Å), Tyr772
BSN-016	-2.27231	Thr85, Thr87, Lys163 (1.80 Å), Gln176, Leu177 (1.94 Å), Phe178, Gly179, Ser180, Asp276, Ile277, Gly614, Phe615, Arg620 ^[c] , Gly621
BSN-017	2.69225	Ser46, Ala47, Ser48, Gln125, Gly126, Gln176, Leu177, Phe178 ^[b] , Ser180, Glu273, Asn274, Ile277, Ala279, Val612, Phe628, Lys770 (2.44 Å)
BSN-018	-7.4936	Ser48, Pro50, Gln125, Leu177, Phe178 ^[c] , Gly179, Ser180, Glu273, Asn274, Ile277, Ala279, Val612, Phe615, Phe628, Lys770 ^[c,c] , Tyr772
BSN-019	-8.54318	Ser48, Gln125, Ser134, Ser135, Gln176, Leu177, Phe178, Gly179, Ser180, Glu273, Asn274, Ile277, Val612, Phe615 ^[b,b] , Phe628, Lys770, Tyr772
BSN-020	-1.1455	Ser48, Pro50, Gln125, Leu177, Gly178, Gly179, Ser180, Glu273, Asn274, Ile277, Ala279, Val612, Phe615, Phe628, Tyr772
BSN-023	-12.7251	Thr44, Gln89, Glu130, Lys131, Ser132, Ser133, Ser134, Gln176, Leu177, Phe178 ^[b] , Gly179, Ile277, Ala279, Lys292 ^[c,c] , Val612, Phe615, Phe628
CIP	-10.1775	Thr87, Gln89, Gln176, Phe178, Gly179, Asn274, Asp276, Ile277, Ala279, Val612, Phe615, Arg620 (1.51 Å), Phe628

^avan der Waals contact distance: <4Å; **H-bonds** indicated in bold text.

^b π - π interactions. ^[c] π -cation interactions. ^[d] π - σ interactions.

half of their concentrations of the observed MIC values (2-fold dilution lower than their MIC value) in combinations with CIP against the same bacterial mutant, a reversal in the antibacterial activity of CIP with up to 10-fold better MIC values was observed, as shown in Table 2. As a result of the measured synergism test of the BSN-coded 2-substituted benzothiazole derivatives, it was found that the compounds holding 4-(4-methylphenylacetamido)phenyl and 4-(phenylpropionamido)phenyl moieties on the 2nd position at the benzothiazole ring, BSN-006 and BSN-023, respectively, provided the most significant contribution in the reversal of antibacterial activity of CIP among the tested compounds.

As shown in Table 2, the tested BSN-coded compounds demonstrated reversal of the antibacterial activity of CIP against the AcrAB-TolC overexpressor *E. coli* AG102 strain, contributing sensitivity on the MIC values of CIP between 2 to 10-fold double dilution better antibacterial activity, except compounds BSN-002 and BSN-008. Among the tested combinations, the compounds BSN-006 and BSN-023 exhibited the most significant reversal

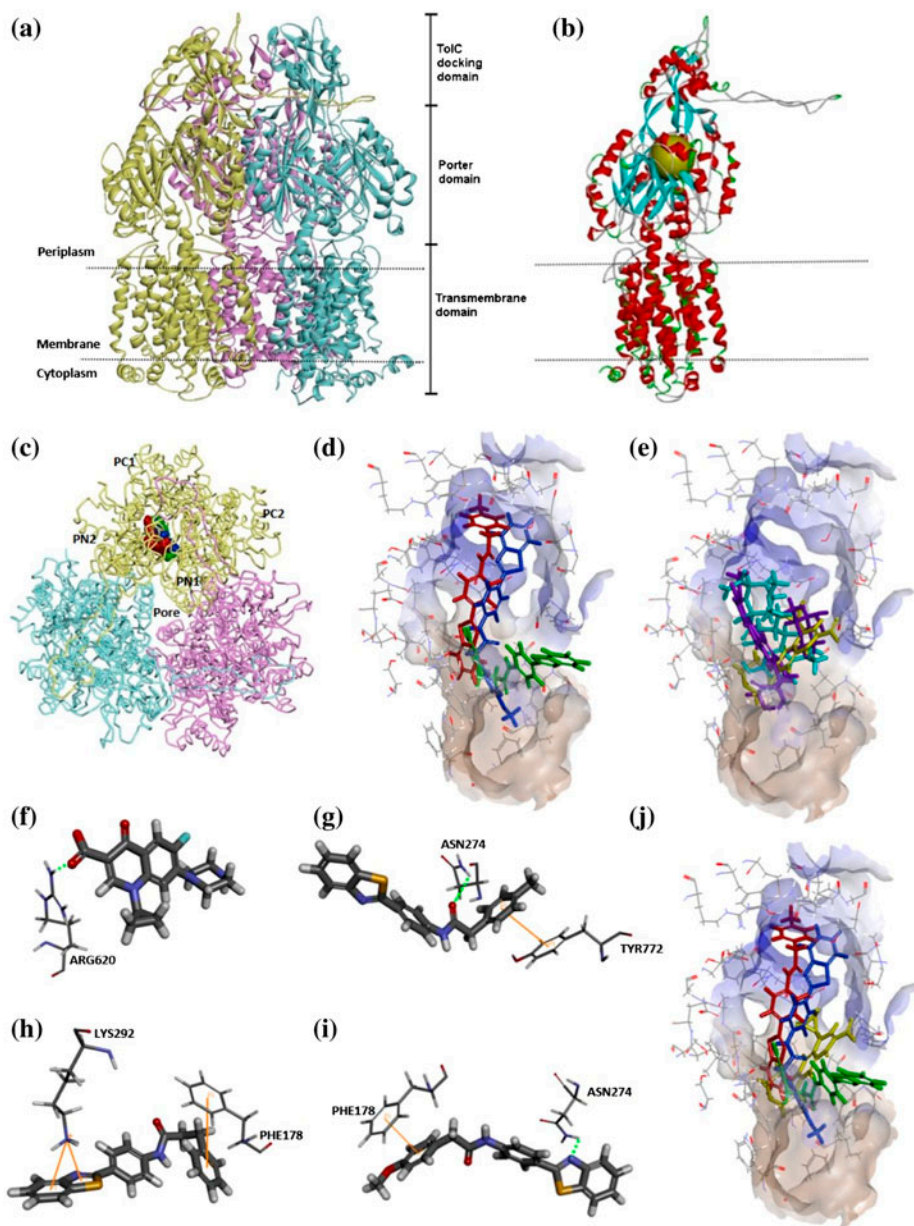
antibacterial activity of CIP against the *E. coli* AG102, providing a MIC value of 0.004 $\mu\text{g/ml}$, which is below the EUCAST susceptibility MIC breakpoint for CIP versus *E. coli* for use in clinical treatment [38]. While the tested compound BSN-008 did not achieve any reversal activity on CIP, interestingly the tested compound BSN-002 determined a MIC value 4-fold higher than CIP. Compound BSN-002 possesses the most lipophilic substituent on its structure among the tested compounds, holding a *sec*-butoxy group ($\text{OCH}(\text{CH}_3)\text{C}_2\text{H}_5$) at the *para* position of the terminal phenyl moiety. Presumably, this compound's higher lipophilicity may be the reason for this outlying result by affecting the inner and/or outer bacterial membranes, which can cause some undesirable effects on the influx of the CIP to the bacterial cell.

3.2 Description of the binding site features of AcrB using molecular docking

The AcrAB-TolC RND efflux pump system of *E. coli* possess tripartite structural organization, as shown in Figure 1(a), which is able to transport diverse structures of compounds out of the bacterial cell, conferring resistance to a broad spectrum of antibiotics. In the AcrAB-TolC tripartite efflux system, AcrB, which cooperates together with TolC and AcrA, designates the substrate specificity and the principal multidrug RND exporter. It provides intrinsic drug tolerance to *E. coli* by extruding a wide variety of compounds directly out of the cell [15].

The RND protein AcrB is composed of 1049 amino acids, and the resolved crystal structure for the AcrB protein holds three AcrB monomers (protomers) organized as a homotrimer [4,57]. Within the asymmetric AcrB trimer, each monomer has a different conformation denoted as loose (L), tight (T), and open (O) (access, binding, and extrusion, respectively) [58]. Each of the protomers is composed of three different domains: a transmembrane (TM) domain, a membrane-proximal pore or porter domain, which is formed from an extended loop connecting TM helices, and a membrane-distal TolC-docking domain (Figure 2(a)). Both the porter domain and the docking domain present mixed α/β -structures, with the porter domain being an $\alpha+\beta$ sandwich with anti-parallel β -sheet, while the docking domains form a unique folded family [15,16,58,59].

As shown in Figure 1(b), the protomer exists as the tight (T) conformation, and has a binding pocket located in the porter domain bound with the substrate, indicated as the binding protomer. The substrate binding pocket examined in the porter domain of the binding protomer revealed that it was enriched with aromatic amino acid residues such as Phe136, Phe178, Phe610, Phe615, Phe617, Phe628, and Tyr772, which interacted with the substrate by hydrophobic or aromatic–aromatic (π – π) interactions. There were also several polar residues in this area, such as Asn274, Gln176, Gly179, Asn274, Arg620, Thr87, Ser180, Glu273, and Asp276, possibly forming hydrogen bonds with the drug molecule [3,4,15,22,60]. This consequence might provide an explanation for AcrB's property of broad spectrum of substrate attraction, whereas different residues were used for binding of different substrates. The second monomer, which exists as the open (O) conformation after extrusion of the substrate, was designated as the extrusion protomer. The third monomer, exhibited as the loose (L) conformation and possessing an empty binding site for the binding of the following substrate, was defined as the access protomer [2–4,15,58,61]. In the access state or the loose (L) conformation, a 'vestibule' near the entrance was open to the periplasm, allowing potential substrates to access the protomer. During the binding, the protomer or tight (T) conformation step, which comprises the binding pocket in the interior of the periplasmic porter domain, achieves the binding of potential substrate to the different sites in the binding pocket [2–4,15,58,61].



The resolved crystal structure of AcrB with its substrates, minocycline (PDB ID: 2DRD) or doxorubicin (PDB ID: 2DR6) demonstrated that only one of the three protomers (the T or binding monomer) showed binding through these low molecular mass substrates (LMMS) within the asymmetric AcrB trimer [3,4,15,61,62]. The minocycline or doxorubicin molecules were bound in the phenylalanine-rich region (Phe136, Phe178, Phe610, Phe615, and Phe618)

in the deep binding pocket at the centre of the porter domain between PC1 and PN2 subdomains of the binding monomer [1,2,22]. Substrates possessing high molecular mass (HMMS), such as rifampicin or erythromycin, bind to the access monomer, and the binding sites are located between PC1 and PC2 in the substrate translocation channel, which is separated from the phenylalanine-rich deep binding pocket (distal pocket) by a switch loop or G-loop (Phe617 loop), and has been shown to be important for substrate adaptation [2,60,62]. Rifampicin or erythromycin first bind to the proximal pocket in the access state and are then forced into the distal pocket in the binding state by a peristaltic mechanism involving subdomain movements that include a shift of the switch loop or G-loop. The path under the switch loop is too narrow for the HMMSs to move into the distal pocket. The switch loop swings during the conformational change from the access stage to the binding stage. HMMSs could be transferred from the proximal pocket to the distal pocket through the swinging of the switch loop and proximal pocket shrinking, followed by distal pocket expansion during the transition from the access to the binding stages [2,62]. Thus, the HMMS binding pocket is referred to as a proximal pocket, and the LMMS binding pocket is referred to as a distal pocket, and substrates possessing high molecular mass (HMMSs), such as rifampicin or erythromycin, first bind to the proximal pocket in the access monomer [3,4,63]. In contrast, low molecular mass substrates (LMMSs), such as CIP, minocycline or doxorubicin, travel through the proximal pocket without specific binding and immediately bind to the distal pocket in the binding monomer [2,4,13,58,62]. The presence of two discrete, high-volume multisite binding pockets contributes to the remarkably broad substrate recognition of AcrB.

Based on this knowledge, we decided to perform our docking studies by using the AcrB binding monomer crystal structure of AcrB (PDB ID: 2DRD) [15], because the tested BSN compounds have low molecular weights (MWs) (of between 330 and 402); CIP, minocycline, and doxorubicin have MWs of 330, 457, and 543, respectively. This is consistent with recent coarse-grained molecular simulations showing that most of the uptake events of relatively



Figure 2. The performed docking poses. (a) The side view of the homotrimer structure of AcrB indicating three distinct domains performed from the crystal structure of AcrB (PDB ID: 2DRD). (b) The side view protomer structure of AcrB showing the selected binding sphere used in our docking studies. (c) The top cut view of homotrimer asymmetric structure of AcrB indicating the protomer distal pocket binding site of the tested compounds BSN-004, BSN-006, and BSN-023 bound at the AcrB binding monomer. (d) The front cut side view of docked compounds BSN-006 (red), BSN-023 (green), and BSN-004 (blue) bound to the distal pocket site of AcrB binding monomer. (e) The front cut side view of the docked CIP (yellow), minocycline (purple), and doxorubicin (cyan) bound to the distal pocket site of AcrB binding monomer. (f) Docked position of CIP: the hydrogen bond performed between the carbonyl oxygen of carboxyl group and Arg620 (green dashed lines). (g) Docked position of BSN-006: The hydrogen bond performed between carbonyl oxygen of amide group substituted to the 2nd position of the benzothiazole ring and Asn274 (green dashed lines) and the π - π interaction achieved between the terminal phenyl ring substituted to the 2nd position of benzothiazole moiety and Tyr772 (brown line). (h) Docked position of BSN-023: two π -cation interactions performed between the benzene and the thiazole rings of the benzothiazole fused system and Lys192 (brown lines) and the π - π interaction performed between the terminal phenyl ring substituted to the 2nd position of the benzothiazole fused system and Phe178 (brown line). (i) Docked position of BSN-004: the hydrogen bond performed between the nitrogen atom of the thiazole ring of the benzothiazole fused system and Asn274 (green dashed lines) and the π - π interaction achieved between the terminal phenyl ring substituted to the 2nd position of benzothiazole moiety and Phe178 (brown line). (j) The front cut side view of docked compounds BSN-006 (red), BSN-023 (green), BSN-004 (blue), and CIP (yellow) bound to the distal pocket site of AcrB binding monomer.

small substrates by AcrB occur from the binding monomer [60]. The binding sphere (coordinates; 168.735, 127.421, 29.5799, radius; 7.62706) in the porter domain elucidated from the crystal structure of AcrB binding monomer was selected from the current selection method by using the DS 3.5 protocol (Figure 2(b)). Our performed docking results have revealed that the tested compounds BSN-004, BSN-006, and BSN-023, which exhibited the most significant potential EPI activities, bound to the distal pocket at the opening edge of the exit channel of the binding site of the AcrB binding monomer (Figure 2(c,d)) similar to how CIP, minocycline, and doxorubicin were bound (Figure 2(e)). This result is in accordance with the literature; both the tested BSN compounds and the appropriate docked antibiotics possess LMMSs bound to the same distal pocket site in the AcrB binding monomer [2,4,15,22,58].

To analyse the binding site features of the tested BSN-coded 2-substituted benzothiazole derivatives, with CIP used as the reference antibiotic substrate, molecular docking studies were performed using CDOCKER [43], and the predicted modes of the interactions between the BSN compounds and CIP are shown in Figure 2(f-i). As shown in Figure 2(f), the antibiotic CIP, which is docked into the distal pocket site of the AcrB binding monomer, possessed a hydrogen bond with the amino acid residue Arg620, and performed interactions with Phe178, Phe615, and Phe628 in the phenylalanine-rich region of the distal binding pocket, having a van der Waals contact distance $<4 \text{ \AA}$ (Table 3, CIP Interacting Residues). When the putative EPI active compounds BSN-006 and BSN-023 docked at the binding site of the AcrB binding monomer, BSN-006 showed a hydrogen bond with Asn274 and π - π interaction with Tyr772 (Figure 2(g)) while BSN-023 achieved π - π interaction with Phe178 and two π -cation interactions with Lys192 (Figure 2(h)). In addition, the other tested potential EPI active compound, BSN-004, displayed a hydrogen bond with the amino acid residue Asn274 and a π - π interaction with Phe178 at the distal binding site of the AcrB binding monomer (Figure 2(i)).

The docked pose of BSN-006 displayed a phenyl trap interaction showing π - π interaction with Tyr772, as well as performing an interaction with Phe178 in the phenylalanine-rich region in the binding monomer distal binding site, with a van der Waals contact distance $<4 \text{ \AA}$ (Table 3, BSN-006 Interacting Residues). Further, the other two putative EPI inhibitors BSN-023 and BSN-004 directly performed π - π interactions with the distal binding pocket phenylalanine-rich region residue Phe178. These performed docking results revealed that the observed putative inhibitors BSN-006, BSN-023, and BSN-004 had affinity to interact with the phenylalanine-rich region in the distal pocket identified in the inhibitor-bound structure of AcrB [2,58,60,62]. Consequently, these new putative BSN inhibitors overlapped with the binding site of the LMMS binding pocket in the AcrB binding monomer (Figure 2(d)), which is CIP, minocycline and doxorubicin bound (Figure 2(e)), while part of the BSN compounds are inserted into a narrow phenylalanine-rich region in the deep binding pocket, termed the hydrophobic trap, suggesting that they competitively inhibit substrate binding and hinder the functional rotation of the efflux pump (Figure 2(j)).

When the docking interactions of the tested BSN compounds were compared with the molecular simulation studies to investigate the putative binding modes of well-known AcrB inhibitors PA β N and NMP [1,22], both PA β N and NMP were predicted to have interactions with the switch loop or G-loop [1]. As discussed in the literature, PA β N and NMP are only partially bound within the hydrophobic trap, and basically are found between this region and the tip of the G-loop [22]. In contrast, our docking results show that the BSN compounds bind to the distal pocket in the binding monomer of AcrB, interacting with the phenylalanine-rich region.

The calculated binding energy scores of CIP, BSN-006, BSN-023, and BSN-004 were calculated as -10.176 , -17.972 , -13.023 , and -7.686 kcal mol⁻¹, respectively (Table 3). These calculated scores also show that the tested compounds BSN-006, BSN-023, and BSN-004 displayed significant binding interaction properties, and that BSN-006 and BSN-023 contained stronger binding energies than CIP; BSN-006 and BSN-023 could be described as the substrates of the AcrB and competitively inhibited the substrate binding site. The binding energy obtained from BSN-004 was found to be lower than the binding energy of CIP. It also showed interactions with the phenylalanine-rich region in the deep distal binding pocket in the AcrB binding monomer, suggesting that it could act as an uncompetitive inhibitor/blocker at the CIP substrate binding site, which may generate some steric hindrance.

On the other hand, the calculated binding energy differences between the compounds BSN-006, BSN-023, and BSN-004 may arise from the dissimilar synergistic activity consequences, and/or because the selected docking pose did not reflect the binding free energies with sufficient accuracy, or because of the complexity of the protein structure. An interesting binding energy range variation was also found among five tested compounds BSN-001, BSN-005, BSN-010, BSN-016, and BSN-017; these BSN compounds have a similar synergistic activity, reducing the MIC value of CIP 4-fold (0.03 $\mu\text{g/ml}$), as shown in Table 2. This may be because the synergism observed in many cases could be attributed to non-specific damage to the bacterial membrane. Compounds that permeabilize the membrane of Gram-negative organisms always show synergism with antibiotics. It is therefore important that potential inhibitors are not only identified on their synergism with antibiotics; additionally subsequent biochemical assays are needed, in which the compounds will be determined as truly acting with efflux inhibitory activity [1].

To determine the correlation between the calculated binding energy scores evaluated from the docked compounds and experimental affinities throughout, a linear regression analysis is adequate, and the quality of the models can be determined on the basis of statistical parameters such as goodness of fit (r^2) [63]. In this context, as shown in the linear regression analysis plot given in Figure 3, our docking results disclosed that the correlation between the

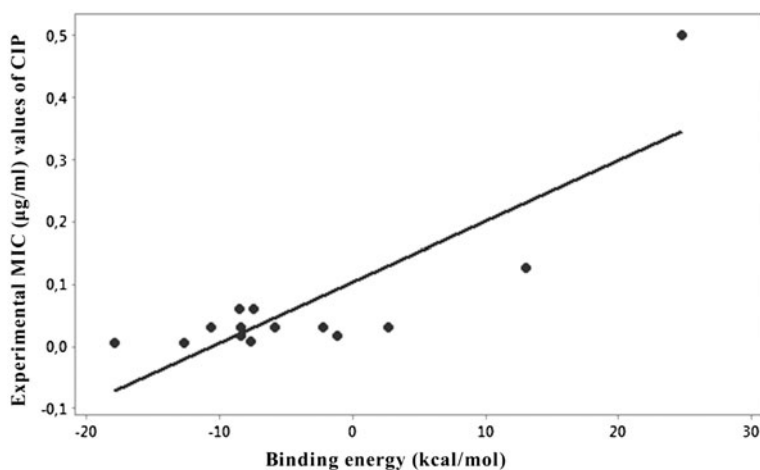


Figure 3. The scattergraph showing the correlation between the calculated binding energy scores evaluated from the docked poses all of the tested BSN compounds versus experimentally measured MIC values of CIP combined with BSN compounds ($r^2 = 0.70$ ($p < 0.001$)).

calculated binding energy scores evaluated from the docked poses of all of the tested BSN compounds given in Table 3 and experimentally measured MIC values of CIP combined with BSN compounds exhibited a r^2 value of 0.70 ($p < 0.001$). The adjusted r^2 coefficient revealed that the calculated binding energy scores of all of the tested BSN compounds exhibited a reliable correlation versus the experimentally observed MIC values of CIP combined with BSN compounds [63].

4. Conclusions

Because conventional antibiotics are becoming increasingly ineffective against pathogenic microorganisms due to the emergence of MDR, there is a crucial requirement to overcome bacterial resistance. Consequently, there is a necessity to use inhibitors of resistance mechanisms, which are able to potentiate the activity of existing antibiotics. Inhibition of MDR efflux pumps in Gram-negative pathogens can restore the antibiotic susceptibility of resistant strains, and might provide a reversal of the clinical activity of current antibiotics. Such inhibitors are expected to decrease the intrinsic resistance of bacteria to antibiotics by using the co-administered antibiotics with inhibitors that neutralize the resistance and, consequently, restore the clinical use of antibiotics in resistant microorganisms.

The use of inhibitors of MDR efflux pumps (EPIs) in combination with antibiotics in an adjuvant therapy has revealed some encouraged results in overcoming the MDR caused by the efflux pumps [23]. This combination can be tested by using an EPI or a substrate of a RND efflux pump at a sub-inhibitory concentration or a dosage less than the inhibitory level (sub-MICs) with an antibiotic [1,64]. Inhibiting/competing with the binding site of the RND efflux pump protein is one of the significant procedures in inhibiting the RND efflux pumps [1,4].

In conclusion, the combined use of EPIs with antibiotics appears to be a promising therapy in the struggle with antibiotic resistance. The development of new inhibitor molecules based on the models generated by the crystal structure of the efflux pumps will allow the generation of more reliable inhibitors which perform a more target-specific inhibition that binds directly to the pump, and therefore blocks it, either in a competitive or a non-competitive manner with the substrates. In accordance with these findings, among BSN-coded 2-substituted benzothiazole derivatives, the tested compounds BSN-006 and BSN-023 reduced the MIC value of CIP against AcrAB-TolC overexpressor *E. coli* AG102 strain 10-fold, while BSN-004 reduced it 8-fold (Table 2), providing MIC susceptibility breakpoint for CIP versus *E. coli*. These results revealed that these tested BSN compounds could be new putative EPIs, showing the ability to restore the antibacterial activity of CIP in the efflux pump of the overexpressor *E. coli* AG102 mutant.

The performed docking poses and the calculated binding energy scores given in Table 3 revealed that BSN-006, BSN-023, and BSN-004 demonstrated significant binding interactions in the binding site of the AcrB binding monomer. Moreover, compounds BSN-006 and BSN-023 possessed stronger binding interaction energies than CIP. These findings verified that BSN-006, BSN-023, and BSN-004 acted as the substrates of the AcrB.

The docking results also revealed that the compounds BSN-004, BSN-006, and BSN-023 bound to the distal pocket site in the AcrB porter domain by inhibiting/blocking the CIP substrate binding site (Figure 2(j)). This may have generated steric hindrance, impairing the antibiotic binding at its affinity site.

Finally, it may be concluded that the performed docking studies, which described the binding site features of tested BSN-coded 2-substituted benzothiazole derivatives on MDR efflux pump AcrB, could provide insights for further studies in order to design new potential EPIs.

Acknowledgment

This study was supported by TUBITAK Project No: 107S455 (SBAG-COST BM0701-19) and EU Framework Program, COST Office, Action BM0701 (ATENS).

Disclosure statement

No potential conflict of interest was reported by the authors.

References

- [1] H. Venter, R. Mowla, T. Ohene-Agyei, and S. Ma, *RND-type drug efflux pumps from Gram-negative bacteria: Molecular mechanism and inhibition*, *Front Microbiol.* 6 (2015), pp. 377.
- [2] A. Yamaguchi, R. Nakashima, and K. Sakurai, *Structural basis of RND-type multidrug exporters*, *Front. Microbiol.* 6 (2015), p. 327.
- [3] J. Sun, Z. Deng, and A. Yan, *Bacterial multidrug efflux pumps: Mechanisms, physiology and pharmacological exploitations*, *Biochem. Biophys. Res. Commun.* 453 (2014), pp. 254–267.
- [4] J. Anes, M.P. McCusker, S. Fanning, and M. Martins, *The ins and outs of RND efflux pumps in Escherichia coli*, *Front. Microbiol.* 6 (2015), pp. 1–11.
- [5] B. Marquez, *Bacterial efflux system and efflux pump inhibitors*, *Biochimie* 87 (2005), pp. 1137–1147.
- [6] P. Wiczorek, P. Sacha, T. Hauschild, M. Zorawski, M. Krawczyk, and E. Tryniszewska, *Multidrug resistant Acinetobacter baumannii – the role of AdeABC (RND family) efflux pump in resistance to antibiotics*, *Folia Histochem. Cytophiol.* 46 (2008), pp. 257–267.
- [7] K. Poole, *Efflux pumps as antimicrobial resistance mechanisms*, *Ann. Med.* 39 (2007), pp. 162–176.
- [8] L.J. Piddock, *Multidrug-resistance efflux pumps? Not just for resistance*, *Nat. Rev. Microbiol.* 4 (2006), pp. 629–636.
- [9] M. Putman, H.W. van Veen, and W.N. Konings, *Molecular properties of bacterial multidrug transporters*, *Microbiol. Mol. Biol. Rev.* 64 (2000), pp. 672–693.
- [10] A. Kumar and H.P. Schweizer, *Bacterial resistance to antibiotics: Active efflux and reduced uptake*, *Adv. Drug Deliv. Rev.* 57 (2005), pp. 1486–1513.
- [11] X.Z. Li and H. Nikaido, *Efflux-mediated drug resistance in bacteria*, *Drugs* 64 (2004), pp. 159–204.
- [12] T. Sato, S. Yokota, T. Okubo, K. Ishihara, H. Ueno, Y. Muramatsu, N. Fujii, and Y. Tamura, *Contribution of the AcrAB-TolC efflux pump to high-level fluoroquinolone resistance in Escherichia coli isolated from dogs and humans*, *J. Vet. Med. Sci.* 75 (2013), pp. 407–414.
- [13] O. Lomovskaya and K.A. Bostian, *Practical applications and feasibility of efflux pump inhibitors in the clinic—a vision for applied use*, *Biochem. Pharmacol.* 71 (2006), pp. 910–918.
- [14] D. Du, Z. Wang, N.R. James, J.E. Voss, E. Klimont, T. Ohene-Agyei, H. Venter, W. Chiu, and B.F. Luisi, *Structure of the AcrAB-TolC multidrug efflux pump*, *Nature* 509 (2014), pp. 512–515.
- [15] S. Murakami, R. Nakashima, E. Yamashita, T. Matsumoto, and A. Yamaguchi, *Crystal structure of multidrug transporter reveal a functionally rotating mechanism*, *Nature* 443 (2006), pp. 173–179.
- [16] J.M. Pages, M. Masi, and J. Barbe, *Inhibitors of efflux pumps in Gram-negative bacteria*, *Trends Molec. Med.* 11 (2005), pp. 382–389.
- [17] J.M. Pages and L. Amaral, *Mechanisms of drug efflux and strategies to combat them: Challenging the efflux pump of Gram-negative bacteria*, *Biochim. Biophys. Acta* 1794 (2009), pp. 826–833.

- [18] C. Kourtesi, A.R. Ball, Y.Y. Huang, S.M. Jachak, D.M.A. Vera, P. Khondkar, S. Gibbons, M.R. Hamblin, and G.P. Tegos, *Microbial efflux systems and inhibitors: Approaches to drug discovery and the challenge of clinical implementation*, *Open Microbiol. J.* 7 (2013), pp. 34–52.
- [19] O. Lomovskaya, M.S. Warren, A. Lee, J. Galazzo, R. Fronko, M. Lee, J. Blais, D. Cho, S. Chamberland, and T. Renau, *Identification and characterization of inhibitors of multidrug resistance efflux pumps in Pseudomonas aeruginosa: Novel agents for combination therapy*, *Antimicrob. Agents Chemother.* 45 (2001), pp. 105–116.
- [20] M. Viveiros, A. Martins, L. Paixão, L. Rodrigues, M. Martins, I. Couto, E. Fahnrich, W.V. Kern, and L. Amaral, *Demonstration of intrinsic efflux activity of Escherichia coli K-12 AG100 by an automated ethidium bromide method*, *Int. J. Antimicrob. Agents* 31 (2008), pp. 458–462.
- [21] R. Misra, K.D. Morrison, H.J. Cho, and T. Khuu, *Importance of real-time assays to distinguish multidrug efflux pump inhibiting and outer membrane destabilizing activities in Escherichia coli*, *J. Bacteriol.* (2015), doi: [10.1128/JB.02456-14](https://doi.org/10.1128/JB.02456-14)[Epub ahead of print].
- [22] A.V. Vargiu, P. Ruggerone, T.J. Opperman, S.T. Nguyen, and H. Nikaido, *Molecular Mechanism of MBX2319 inhibition of Escherichia coli AcrB multidrug efflux pump and comparison with other inhibitors*, *Antimicrob. Agents Chemother.* 58 (2014), pp. 6224–6234.
- [23] J.A. Bohnert and W.V. Kern, *Selected arylpiperazines are capable of reversing multidrug resistance in Escherichia coli overexpressing RND efflux pumps*, *Antimicrob. Agents Chemother.* 49 (2005), pp. 849–852.
- [24] W.V. Kern, P. Steinke, A. Schumacher, S. Schuster, H. von Baum, and J.A. Bohnert, *Effect of 1-(1-naphthylmethyl)-piperazine, a novel putative efflux pump inhibitor, on antimicrobial drug susceptibility in clinical isolates of Escherichia coli*, *J. Antimicrob. Chemother.* 57 (2006), pp. 339–343.
- [25] S. Yilmaz, G. Altinkanat-Gelmez, K. Bolelli, D. Guneser-Merdan, M.U. Over-Hasdemir, I. Yildiz, E. Aki-Yalcin, and I. Yalcin, *Pharmacophore generation of 2-substituted benzothiazoles as adeabc efflux pump inhibitors in A. baumannii*, *SAR QSAR Environ. Res.* 25 (2014), pp. 551–563.
- [26] S. Cagnacci, L. Gualco, E. Debbia, G.C. Schito, and A. Marchese, *European emergence of ciprofloxacin-resistant Escherichia coli clonal groups O25:H4-ST 131 and O15:K52:H1 causing community-acquired uncomplicated cystitis*, *J. Clin. Microbiol.* 46 (2008), pp. 2605–2612.
- [27] World Health Organization (WHO). *Antimicrobial Resistance: Global Report on Surveillance 2014*. WHO, Geneva, 2014.
- [28] S. Yilmaz, I. Yalcin, F. Kaynak-Onurdag, S. Ozgen, I. Yildiz, and E. Aki, *Synthesis and in vitro antimicrobial activity of novel 2-(4-(substituted-carboxamido)benzyl/phenyl)benzothiazoles*, *Croat. Chem. Acta.* 86 (2013), pp. 223–231.
- [29] K. Bolelli, I. Yalcin, T. Ertan-Bolelli, S. Ozgen, F. Kaynak-Onurdag, I. Yildiz, and E. Aki, *Synthesis of novel 2-[4-(4-substitutedbenzamido/phenylacetamido)phenyl]benzothiazoles as antimicrobial agents*, *Med. Chem. Res.* 21 (2012), pp. 3818–3825.
- [30] C.A. Elkins and L.B. Mullis, *Substrate competition studies using whole-cell accumulation assays with the major tripartite multidrug efflux pumps of Escherichia coli*, *Antimicrob. Agents Chemother.* 51 (2007), pp. 923–929.
- [31] M. Fadli, J. Chevalier, A. Saad, N.E. Mezrioui, L. Hassani, and J.M. Pages, *Essential oils from Moroccan plants as potential chemosensitisers restoring antibiotic activity in resistant Gram-negative bacteria*, *Int. J. Antimicrob. Agents* 38 (2011), pp. 325–330.
- [32] A.M. George and S.B. Levy, *Amplifiable resistance to tetracycline, chloramphenicol, and other antibiotics in Escherichia coli: Involvement of a non-plasmid-determined efflux of tetracycline*, *J. Bacteriol.* 155 (1983), pp. 531–540.
- [33] Z. Shaohua, J.J. Maurer, S. Hubert, J.F. De Villena, P.F. McDermott, J. Meng, S. Ayers, L. English, and D.G. White, *Antimicrobial susceptibility and molecular characterization of avian pathogenic Escherichia coli isolates*, *Vet. Microbiol.* 107 (2005), pp. 215–224.
- [34] P.S. Cohen, L.M. McMurry, and S.B. Levy, *marA locus causes decreased expression of OmpF porin in multiple-antibiotic-resistant (Mar) mutants of Escherichia coli*, *J. Bacteriol.* 170 (1988), pp. 5416–5422.

- [35] H. Okusu, D. Ma, and H. Nikaido, *AcrAB efflux pump plays a major role in the antibiotic resistance phenotype of Escherichia coli multiple-antibiotic-resistance (Mar) mutants*, J. Bacteriol. 178 (1996), pp. 306–308.
- [36] D.G. White, J.D. Goldman, B. Demple, and S.B. Levy, *Role of the acrAB locus in organic solvent tolerance mediated by expression of marA, soxS, or robA in Escherichia coli*, J. Bacteriol. 179 (1997), pp. 6122–6126.
- [37] Clinical and Laboratory Standards Institute (CLSI) (formerly NCCLS), *Performance standards for antibacterial susceptibility testing*, 16th Informational Supplement, CLSI M100-S016, Clinical and Laboratory Standards Institute, 940 West Valley Road, Wayne, PA, 2006.
- [38] European Committee on Antimicrobial Susceptibility Testing (EUCAST AST guidelines), Breakpoint tables for interpretation of MICs and zone diameters. Version 1.3 December 2010.
- [39] Discovery Studio 3.5, Accelrys Software Inc., San Diego 2013; software available at <http://accelrys.com/products/discovery-studio>.
- [40] B.R. Brooks, R.E. Bruccoleri, B.D. Olafson, D.J. States, S. Swaminathan, and M. Karplus, *CHARMM: A program for macromolecular energy, minimization, and dynamics calculations*, J. Comput. Chem. 4 (1983), pp. 187–217.
- [41] E. Aki-Yalcin, T. Ertan-Bolelli, T. Taskin-Tok, O. Ozturk, S. Ataei, C. Ozen, I. Yildiz, and I. Yalcin, *Evaluation of inhibitory effects of benzothiazole and 3-aminobenzothiazolium derivatives on DNA topoisomerase II by molecular modeling studies*, SAR QSAR Environ. Res. 25 (2014), pp. 637–649.
- [42] C. Brooks, *III assessing, improving and using grid-based docking algorithms in CHARMM*, Abstracts of Papers, Proceedings of the 233rd National Meeting and Exposition of the American Chemical Society, Chicago, IL, 25–29 March 2007, Abstract COMP-250.
- [43] G. Wu, D.H. Robertson, C.L. III. Brooks, and M. Vieth, *Detailed analysis of grid-based molecular docking: A case study of CDOCKER – A CHARMM-based MD docking algorithm*, J. Comput. Chem. 24 (2003), pp. 1549–1562.
- [44] P.D. Lyne, M.L. Lamb, and J.C. Saeh, *Accurate prediction of the relative potencies of members of a series of kinase inhibitors using molecular docking and MM-GBSA scoring*, J. Med. Chem. 49 (2006), pp. 4805–4808.
- [45] N. Moitessier, P. Englebienne, D. Lee, J. Lawandi, and C.R. Corbeil, *Towards the development of universal, fast and highly accurate docking/scoring methods: A long way to go*, Br. J. Pharmacol. 153(Suppl. 1) (2008), pp. S7–S26.
- [46] F.A. Momany and R. Rone, *Validation of the general purpose QUANTA 3.2/CHARMM force field*, J. Comput. Chem. 13 (1992), pp. 888–900.
- [47] B. Jayaram, D. Sprous, and D.L. Beveridge, *Solvation free energy of biomacromolecules: Parameters for a modified generalized born model consistent with the AMBER force field*, J. Phys. Chem. B 102 (1998), pp. 9571–9576.
- [48] I. Massova and P.A. Kollman, *Combined molecular mechanical and continuum solvent approach (MM-PBSA/GBSA) to predict ligand binding*, Perspect. Drug Discov. 18 (2000), pp. 113–135.
- [49] J. Srinivasan, T.E. III. Cheatham, P. Cieplak, P.A. Kollman, and D.A. Case, *Continuum solvent studies of the stability of DNA, RNA, and phosphoramidate-DNA helixes*, J. Am. Chem. Soc. 120 (1998), pp. 9401–9409.
- [50] P. Gilbert and A.J. McBain, *Biocide usage in the domestic setting and concern about antibacterial and antibiotic resistance*, J. Infect. 43 (2001), pp. 85–91.
- [51] I. Hutchinson, S.A. Jennings, B.R. Vishnuvajjala, A.D. Westwell, and M.F.G. Stevens, *Antitumor benzothiazoles. 16.1 synthesis and pharmaceutical properties of antitumor 2-(4-aminophenyl)benzothiazole amino acid prodrugs*, J. Med. Chem. 45 (2001), pp. 744–747.
- [52] T. Taskin, S. Yilmaz, I. Yildiz, I. Yalcin, and E. Aki, *Insight into eukaryotic topoisomerase II-inhibiting fused heterocyclic compounds in human cancer cell lines by molecular docking*, SAR QSAR Environ. Res. 23 (2012), pp. 345–355.
- [53] R.K. Plemper, K.J. Erlandson, A.S. Lakdawala, A. Sun, A. Prussia, J. Boonsombat, E. Aki-Sene, I. Yalcin, I. Yildiz, O. Temiz-Arpaci, B. Tekiner, D.C. Liotta, J.P. Snyder, and R.W. Compans, *A target*

- site for template-based design of measles virus entry inhibitors, Proc. Natl Acad. Sci. USA 101 (2004), pp. 5628–5633.
- [54] M. Arisoy, O. Temiz-Arpaci, I. Yildiz, F. Kaynak-Onurdag, E. Aki, I. Yalcin, and U. Abbasoglu, *Synthesis, antimicrobial activity and QSAR studies of 2,5-disubstituted benzoxazoles*, SAR QSAR Environ. Res. 19 (2008), pp. 589–612.
- [55] Y. Ugur and A. Akbay, Yarpuzlu, A. Nazikoglu, E. Asan, I. Yildiz, and S. Keles, *Investigating toxic effects of the HIV-RT inhibitor 2-phenoxyethyl-5-chloro-benzimidazole on rat liver*, Turk. J Med. Sci. 35 (2005), pp. 5–12.
- [56] C.A. Lipinski, F. Lombardo, B.W. Dominy, and P.J. Feeney, *Experimental and computational approaches to estimate solubility and permeability in drug discovery and development q settings*, Adv. Drug Deliv. Rev. 46 (2001), pp. 3–26.
- [57] T. Hisano, M. Ichikawa, K. Tsumoto, and M. Tasaki, *Synthesis of benzoxazoles, benzothiazoles and benzimidazoles and evaluation of their antifungal, insecticidal and herbicidal activities*, Annual Report of the Faculty of Pharmacy & Pharmaceutical Sciences, Fukuyama University 1 (1982), pp. 17–25.
- [58] T. Eicher, H.J. Cha, M.A. Seeger, L. Brandstätter, J. El-Delik, J.A. Bohnert, W.V. Kern, F. Verrey, M.G. Grütter, K. Diederichs, and K.M. Pos, *Transport of drugs by the multidrug transporter AcrB involves an access and a deep binding pocket that are separated by a switch-loop*, Proc. Natl Acad. Sci. USA 109 (2012), pp. 5687–5692.
- [59] F. Husain and H. Nikaïdo, *Substrate path in the AcrB multidrug efflux pump of Escherichia coli*, Mol. Microbiol. 78 (2010), pp. 320–330.
- [60] P. Ruggerone, S. Murakami, K.M. Pos, and A.V. Vargiu, *RND efflux pumps: Structural information translated into function and inhibition mechanisms*, Curr. Top Med. Chem. 13 (2013), pp. 3079–3100.
- [61] R. Misra and V.N. Bavro, *Assembly and transport mechanism of tripartite drug efflux systems*, Biochim. Biophys. Acta 1794 (2009), pp. 817–825.
- [62] R. Nakashima, K. Sakurai, S. Yamasaki, K. Nishino, and A. Yamaguchi, *Structures of the multidrug exporter AcrB reveal a proximal multisite drug-binding pocket*, Nature 480 (2011), pp. 565–569.
- [63] V.M. Popov, W.A. Yee, and A.C. Anderson, *Towards in silico lead optimization: Scores from ensembles of protein/ligand conformations reliably correlate with biological activity*, Proteins Struct. Funct. Bioinf. 66 (2007), pp. 375–387.
- [64] N.G. Coldham, M. Webber, M.J. Woodward, and L.J.V. Piddock, *A 96-well plate fluorescence assay for assessment of cellular permeability and active efflux in Salmonella enterica serovar Typhimurium and Escherichia coli*, J. Antimicrob. Chemother. 65 (2010), pp. 1655–1663.